

<https://doi.org/10.1038/s41531-025-01013-z>

# Neural basis of dysexecutive and visuospatial impairments in Parkinson's disease with MCI: a task-based fNIRS study

Check for updates

Hai-Yang Wang<sup>1,2,3</sup>, Lu Ren<sup>1</sup>, Zhongrui Yan<sup>2</sup>, Tingting Zhou<sup>1</sup> & Zhanhua Liang<sup>1</sup>

Parkinson's disease with mild cognitive impairment (PD-MCI) includes various cognitive deficits, classified into two subtypes based on the “dual syndrome hypothesis”: the executive-dominant dopamine pathway dysfunction impairing executive and language functions (PD-EL subtype), and the visuospatial-dominant non-dopaminergic dysfunction affecting visuospatial perception, attention, and memory (PD-VAM subtype). This study involved 182 participants (122 PD, 60 controls) undergoing cognitive assessments. Using PD-MCI Level II criteria, patients were categorized as PD with normal cognition (PD-NC, 48), PD-EL (34), or PD-VAM (40). Functional near-infrared spectroscopy measured brain activation during verbal fluency (executive) and line orientation (visuospatial) tasks. PD-EL showed lower word accuracy and reduced activation in dorsolateral/ventrolateral prefrontal cortices, supplementary motor area, and orbitofrontal cortex compared to PD-NC. PD-VAM had lower line orientation scores and reduced ventrolateral prefrontal activation. These findings suggest that PD-MCI subtypes may exhibit differential neural activation patterns reflecting their cognitive deficits, underscoring the need for targeted interventions and mechanistic research.

Mild cognitive impairment in Parkinson's disease (PD-MCI) stands out as one of the most prevalent and significant cognitive impairments within the PD spectrum<sup>1</sup>. Its prevalence reaches as high as 40%<sup>2</sup>, with an incidence of 20–30% among recently diagnosed PD<sup>3</sup>. Research findings underscore PD-MCI as a distinct predictor for Parkinson's disease dementia (PDD)<sup>4</sup>, with approximately 80% of individuals with PD-MCI eventually developing PDD<sup>5</sup>. This profoundly affects the daily functioning and well-being of individuals with PD. Therefore, investigating early PD-MCI diagnosis bears vital clinical importance, shedding light on cognitive decline mechanisms and guiding the discovery of novel therapeutic targets.

PD-MCI, as a markedly heterogeneous group, presents a significant challenge in current clinical diagnosis and treatment<sup>6</sup>. It arises from pathogenic alterations in distinct neurotransmitter pathways, primarily involving two routes: the dopaminergic-dependent fronto-striatal pathway, and non-dopaminergic pathways encompassing the cholinergic and noradrenergic systems<sup>6</sup>. Expanding on this, the influential “dual syndrome hypothesis” proposes two subtypes of PD-MCI: the dysexecutive subtype, associated with dopaminergic pathway dysfunction and impairments in

executive and language functions (PD-EL), and the visuospatial dysfunction–featured subtype, linked to non-dopaminergic dysfunction with impairments in visuospatial perception, attention, and memory (PD-VAM)<sup>7,8</sup>.

Advanced neuroimaging techniques are at the forefront of studying the neural mechanisms behind PD-MCI. Limited research has explored the pathophysiology of dysexecutive and visuospatial dysfunction subtypes. Resting-state fMRI studies reveal distinct patterns: dysexecutive subtype correlates with decreased functional connectivity (FC) in the sensorimotor network, while visuospatial dysfunction subtype is associated with altered FC in the central executive and temporal networks<sup>9</sup>. Independent component analysis additionally shows heightened FC in the basal ganglia network in visuospatial dysfunction subtype. Dysexecutive subtype, compared to cognitively normal PD and visuospatial dysfunction subtype, exhibits lowered FC in various networks<sup>10</sup>. Betrouni et al. employed electroencephalography to identify spectral and functional alterations in dysexecutive subtype patients, characterized by elevated  $\theta$  and  $\delta$  power, reduced  $\beta 2$  power, and altered FC in the  $\beta 2$  band. Visuospatial dysfunction subtype

<sup>1</sup>Department of Neurology, The First Affiliated Hospital of Dalian Medical University, Dalian, China. <sup>2</sup>Department of Neurology, Jining No. 1 People's Hospital, Shandong First Medical University, Jining, China. <sup>3</sup>Medical Integration and Practice Center, Cheeloo College of Medicine, Shandong University, Jinan, China. ✉e-mail: [tingtingzhou1987@163.com](mailto:tingtingzhou1987@163.com); [liangzhanhua@dmu.edu.cn](mailto:liangzhanhua@dmu.edu.cn)

patients show no similar changes<sup>11</sup>. While these studies shed light on the pathophysiological mechanisms underlying both PD-MCI subtypes from the perspective of resting-state brain networks and EEG, they primarily focus on brain function during rest. Thus, understanding how cognitive neural activity patterns in PD-MCI patients respond to real-world stimuli necessitates task-related studies for more profound insights into these distinct subtypes.

Within the dual syndrome hypothesis framework, both dopaminergic and cholinergic pathways converge onto the prefrontal cortex (PFC)<sup>7,8,12</sup>. The PFC, a central hub orchestrating cognitive activities across the brain, assumes a critical role in advanced cognitive functions like response inhibition, visuospatial processing, and selective attention; impairments in PFC function have implications for a spectrum of neurological disorders<sup>13</sup>, and can lead to executive dysfunction<sup>14</sup>.

Historically, visuospatial function research primarily focused on the posterior cortex, exploring the impact of parietal lobe lesions on visuospatial capabilities<sup>15,16</sup>. However, in recent years, the involvement of the PFC in visuospatial functions has emerged. Neurophysiological studies in non-human primates revealed that when predicting visuospatial information using shape cues, electroencephalographic signals predominantly emanate from the ventrolateral PFC (VLPFC). Conversely, when predicting shape information using visuospatial cues, signals mainly originate from the dorsolateral PFC (DLPFC)<sup>17</sup>. These findings indicate that visuospatial and shape information are relayed through visual pathways to the DLPFC and VLPFC, which mutually process the information, thereby representing visuospatial functions in the lateral PFC<sup>17</sup>. In line with these studies, lesions in the dorsal PFC have been demonstrated to result in impairments in visuospatial memory, while damage to the ventral PFC leads to deficits in shape working memory<sup>18</sup>. In humans, the role of the PFC, particularly the DLPFC and VLPFC, in processing visuospatial information is significant<sup>19</sup>. Moreover, patients with damage to the VLPFC and DLPFC exhibit marked functional deficits in spatial tasks<sup>20</sup>. Brain network studies suggest that the PFC, as a component of the frontoparietal network, is implicated in visuospatial deficits in PD patients with cognitive impairment<sup>8</sup>. Additionally, the VLPFC emerges as a pivotal brain region for visuospatial attention functions<sup>8,21</sup>. These studies collectively underscore that the PFC not only acts as a hub for cholinergic pathway activity but also serves as a crucial region for representing visuospatial functions. Nonetheless, investigations into the neuroimaging mechanisms governing PFC visuospatial functions in PD-MCI patients remain largely unexplored.

fMRI is an indispensable tool for exploring the neurobiological basis of cognitive impairments in specific populations<sup>10</sup>. Nevertheless, when investigating PD-MCI, fMRI faces limitations. It demands strict postural constraints on Parkinson's patients, presenting challenges for severely affected individuals' participation and potentially creating disparities between clinical research and real-world situations. Additionally, fMRI's lower spatial resolution and susceptibility to noise interference, coupled with the mutual influences of environmental and individual factors on PD-MCI patients during tasks, hinder precise control and introduce significant result variations.

The optical technique of functional near-infrared spectroscopy (fNIRS), which monitors alterations in concentrations of oxygenated and deoxygenated hemoglobin in brain tissue<sup>22</sup>. Unlike fMRI, fNIRS is insensitive to motion artifacts and demands less stringent postural requirements from subjects. Furthermore, fNIRS demonstrates high consistency with fMRI in detection outcomes<sup>23</sup>. Considering that PD patients often exhibit tremors and motor impairments, and given that fNIRS imposes fewer restrictions regarding posture, tremors, and movement, it emerges as a highly promising technique for investigating brain function in PD research<sup>22,24</sup>.

Given the increasing importance of understanding PD-MCI's cognitive profiles, this study employs task-based fNIRS to examine behavioral traits and prefrontal activation in two cognitive subtypes: PD-EL and PD-VAM. We hypothesize that, compared to cognitively unimpaired PD patients, the PD-EL subtype will show decreased activation in a broad range

of PFC regions during executive tasks. In contrast, the PD-VAM subtype is expected to exhibit reduced activation in visuospatial-related regions, such as the VLPFC and DLPFC, specifically during visuospatial tasks. These findings will highlight subtle differences in their neural activation profiles.

## Results

### Participants characteristics

122 PD patients and 60 locally matched healthy individuals from the same area were included. Both groups exhibited no significant differences in age, gender, education years, or BMI values (all  $p > 0.05$ ) (Table 1), indicating a strong demographic match. This allows for subtyping of PD-MCI based on cognitive domain assessments in the healthy individuals group.

### Local healthy individuals' cognitive domain assessment

In the local healthy population, the mean and standard deviation for the measurements of the five major cognitive domains are provided in Table 2.

### Demographic, clinical, and cognitive profiles

Cognitive subtyping was conducted on the final cohort of 122 PD patients, utilizing cognitive assessments from the local healthy population and guided by the dual syndrome hypothesis. The results categorized the patients into three groups: 48 PD-NC, 34 PD-EL, and 40 PD-VAM. No statistically significant differences in age, gender, years of education, or BMI values were observed among the three groups ( $p > 0.05$ ). Clinical symptom assessments, including H-Y stage, MDS-UPDRS III, PD duration, and LEDD, also showed no statistical differences ( $p > 0.05$ ). Psychometric evaluations indicated a gradual increase in HAMA and HAMD scores across the three groups (PD-NC < PD-EL < PD-VAM). However, these differences did not reach statistical significance ( $p = 0.111$  and  $p = 0.110$ ). Significantly, the PD-VAM subtype showed lower overall cognitive scores compared to PD-EL and PD-NC. It also demonstrated a higher number of impaired cognitive domains, each associated with lower scores. The results of the analysis of variance and post hoc tests are provided in Table 3 for reference.

### Verbal fluency task

In the task phase, PD-NC exhibited  $9.5 \pm 3.6$  correct word completions, whereas PD-EL showed  $7.3 \pm 3.0$ , signifying a notable statistical distinction ( $p = 0.006$ ). For a detailed visual representation, consult Fig. 1A.

In the VFT task, both groups exhibited distinct patterns of brain activation. The PD-NC group showed enhanced activation in bilateral DLPFC, VLPFC, IPL, SMA, TL, left OFC, and mPFC (Ch8-13, Ch18-25, Ch28-35, Ch37-45, and Ch48-52) ( $p \leq 0.0101$ , FDR corrected) (Fig. 1B). Conversely, the PD-EL group demonstrated increased activation in bilateral VLPFC, TL, and left OFC (Ch23, Ch32-34, Ch40, Ch43-45, Ch49-51) ( $p \leq 0.0087$ , FDR corrected) (Fig. 1C). Intergroup VFT activation comparisons revealed reduced activation in bilateral DLPFC, VLPFC, SMA, left OFC, left IPL, and mPFC for the PD-EL group compared to the PD-NC group (Ch2, Ch8-10, Ch18, Ch21, Ch23, Ch25, Ch29, Ch34, Ch35, Ch37, Ch39, Ch45, Ch48, Ch50) ( $p \leq 0.0150$ , FDR corrected), consistent with Fig. 1D and Table 4. Importantly, these activation patterns were in line with behavioral data; specifically, reduced brain activation during VFT performance was linked to a decrease in the number of words generated. No linear correlation was observed between behavior and brain activation.

### Line orientation task

Behavioral RMANOVA indicated significant main effects for condition ( $F_{1,86} = 79.72$ ,  $p < 0.0001$ , partial  $\eta^2 = 0.48$ ) and group ( $F_{1,86} = 32.172$ ,  $p < 0.0001$ , partial  $\eta^2 = 0.27$ ), as well as a significant interaction between group and condition ( $F_{1,86} = 24.90$ ,  $p < 0.0001$ , partial  $\eta^2 = 0.22$ ) (see Fig. 2A–C). Simple effect analysis revealed that in Line Orientation, PD-NC significantly outperformed PD-VAM ( $p < 0.0001$ ), while no significant difference was observed in the Color Naming task ( $p = 0.113$ ). Post hoc analysis indicated that both PD-NC and PD-VAM groups demonstrated lower accuracy in the LOT compared to the Color Naming task ( $p < 0.01$ ).

**Table 1 | Demographic matching between enrolled local healthy population and PD patients**

	Healthy population <i>n</i> = 60	PD <i>n</i> = 122	<i>P</i> value
Demographics			
Age (years)	62.9 ± 9.1	63.9 ± 7.3	0.242
Gender (male/female)	28/32	68/54	0.249
Education in years	10.5 ± 3.3	11.2 ± 3.3	0.204
BMI	24.6 ± 2.4	24.2 ± 2.9	0.356

Moreover, PD-NC exhibited higher overall accuracy than PD-VAM ( $p < 0.0001$ ).

The 2×2×52 RMANOVA design for brain activation yielded significant main effects for condition ( $F_{1,86} = 22.81$ ,  $p < 0.0001$ , partial  $\eta^2 = 0.21$ ) (Fig. 2D), group ( $F_{1,86} = 8.392$ ,  $p = 0.005$ , partial  $\eta^2 = 0.089$ ) (Fig. 2E), and channel ( $F_{9,6,824.1} = 4.665$ ,  $p < 0.0001$ , partial  $\eta^2 = 0.051$ ). However, interaction effects for group×condition (Fig. 2F), group×channel, and condition×channel were non-significant ( $p > 0.05$ ). Post hoc comparisons revealed that in the Line Orientation, the PD-NC group demonstrated significant enhanced activation in bilateral DLPFC, bilateral VLPFC, bilateral SMA, bilateral OFC, left IPL, right TL, and mPFC (channels 2–4, 7, 10, 12, 13, 15, 18, 19, 21–35, 37–46, 49–52) ( $p \leq 0.0344$ , FDR corrected), whereas the PD-VAM group only exhibited significantly enhanced activation in the right OFC ( $p = 0.0002$ , FDR corrected) (Fig. 2G). However, in the Color Naming task, there was no significant difference in brain activation between the PD-NC and PD-VAM groups ( $p > 0.05$ ) (Fig. 2H). Moreover, intergroup comparisons in the Line Orientation revealed that compared to the PD-NC group, the PD-VAM group displayed significantly reduced activation in bilateral VLPFC (channels 34, 45, and 50) and left DLPFC (channel 27) ( $p \leq 0.0066$ , FDR corrected; Fig. 2I, Table 4). These neuroimaging findings are consistent with the behavioral data, indicating that patients exhibited reduced brain activation during LOT performance, which corresponded with a decrease in accuracy on LOT behavioral tasks. No linear correlation was found between behavior and brain activation.

Discussion

In current PD-MCI research, there has been a predominant focus on resting-state brain activation patterns. However, understanding how PD-MCI patients engage with real-world stimuli necessitates task-related activation studies. Using fNIRS technology, we investigated whether PD-MCI subtypes, defined by the dual syndrome hypothesis, exhibit specific deficits in brain region activation. For the first time, we observed that PD-EL patients, relative to PD-NC, showed reduced activation in the DLPFC, VLPFC, SMA, mPFC, left OFC, and left IPL during an executive task. Conversely, PD-VAM patients exhibited decreased activation primarily in the VLPFC and left DLPFC during a visual spatial task compared to PD-NC. Notably, the neural activation patterns in these tasks closely paralleled behavioral outcomes.

In the VFT analysis, PD-EL patients demonstrated significantly reduced correct word counts compared to PD-NC, indicating impaired language organization and fluency, consistent with prior studies<sup>25</sup>. PD-MCI patients exhibited deficits in word generation and switching during VFT<sup>25</sup>. Early-stage PD may present with deficiencies in semantic and phonemic fluency, characterized by challenges in word retrieval, sentence repetition, and word errors<sup>26</sup>, indicative of executive function abnormalities<sup>25</sup>. Notably, studies have underscored the crucial role of the PFC in tasks involving executive functions<sup>27</sup>, with our fNIRS results revealing widespread PFC underactivation in PD-EL patients during VFT tasks, spanning DLPFC, VLPFC, SMA, IPL, and OFC, aligning with behavioral results and confirming executive function deficits.

Executive control, a complex higher-order cognitive function, relies on coordinated activity across various brain regions. The DLPFC, pivotal for

**Table 2 | Mean and Standard Deviation of ten cognitive tests across five cognitive domains in the local healthy population**

	Executive functions		Language		Visuospatial functions		Attention		Episodic memory	
	Clock Drawing Test	Category Fluency Test (animals)	Similarities Test	30-item Boston Naming Test	Block Design Test	Clock copying (Royall's CLOX)	Digit Span Test	Symbol Digit Test	Auditory Verbal Learning Test	Logical memory
Number	60	60	60	60	60	60	60	60	60	60
Mean	9.13	20.18	18.57	25.08	30.60	14.70	14.30	36.88	35.37	11.71
Standard Deviation	1.31	5.74	3.75	2.29	6.67	1.12	2.68	13.55	8.41	3.70

**Table 3 | Demographic and clinical characteristics, as well as cognitive test performance of the study cohort**

	PD-NC (n = 48)	PD-EL (n = 34)	PD-VAM (n = 40)	P value	Post hoc test
<b>Demographics</b>					
Age (years)	62.9 ± 7.5	64.4 ± 7.5	64.8 ± 6.8	0.439	NA
Gender (male/female)	29/19	15/19	24/16	0.275	NA
Education in years	11.7 ± 2.7	11.5 ± 3.1	10.4 ± 3.5	0.108	NA
BMI	24.3 ± 2.9	23.5 ± 3.3	24.6 ± 2.7	0.228	NA
<b>Clinical data</b>					
Disease Duration (Months)	56.3 ± 31.4	54.4 ± 29.3	49.7 ± 32.4	0.604	NA
Hoehn and Yahr stage	2.1 ± 0.6	2.0 ± 0.5	2.0 ± 0.6	0.578	NA
MDS-UPDRS III	32.8 ± 17.9	31.3 ± 14.7	31.5 ± 15.9	0.911	NA
<b>Medication</b>					
LEDD (mg/day)	437.7 ± 299.9	420.4 ± 230.6	398.8 ± 210.4	0.775	NA
<b>Neuropsychiatric assessment</b>					
HAMA	6.0 ± 4.6	7.1 ± 4.6	8.2 ± 5.6	0.111	NA
HAMD	6.8 ± 4.6	7.5 ± 4.3	9.0 ± 5.8	0.110	NA
<b>Overall efficiency</b>					
MMSE	28.4 ± 1.2	26.6 ± 1.3	25.6 ± 1.9	<0.001	PD-NC > PD-EL; PD-NC > PD-VAM; PD-EL > PD-VAM
MoCA	26.0 ± 1.6	23.0 ± 2.6	20.6 ± 3.2	<0.001	PD-NC > PD-EL; PD-NC > PD-VAM; PD-EL > PD-VAM
<b>Executive functions</b>					
Clock Drawing Test	9.1 ± 0.9	7.1 ± 1.7	8.4 ± 1.1	<0.001	PD-NC > PD-EL; PD-VAM > PD-EL
Category Fluency Test (animals)	18.6 ± 4.7	14.3 ± 3.7	16.6 ± 3.4	<0.001	PD-NC > PD-EL
<b>Episodic memory</b>					
Logical memory	10.7 ± 3.7	9.8 ± 2.9	5.5 ± 2.9	<0.001	PD-NC > PD-VAM; PD-EL > PD-VAM
Auditory Verbal Learning Test	32.8 ± 6.7	31.7 ± 6.3	19.6 ± 6.4	<0.001	PD-NC > PD-VAM; PD-EL > PD-VAM
<b>Visuospatial functions</b>					
Clock copying (Royall's CLOX)	14.9 ± 0.9	14.4 ± 1.0	12.6 ± 2.3	<0.001	PD-NC > PD-VAM; PD-EL > PD-VAM
Block Design Test	29.5 ± 6.0	27.0 ± 3.2	22.5 ± 6.9	<0.001	PD-NC > PD-VAM; PD-EL > PD-VAM
<b>Language</b>					
30-item Boston Naming Test	24.7 ± 1.8	21.6 ± 3.0	23.0 ± 1.9	<0.001	PD-NC > PD-EL; PD-NC > PD-VAM; PD-EL < PD-VAM
Similarities Test	17.5 ± 2.9	14.7 ± 4.7	15.5 ± 2.9	0.001	PD-NC > PD-EL; PD-NC > PD-VAM
<b>Attention/working memory</b>					
Symbol Digit Test	33.1 ± 10.8	29.4 ± 8.7	25.0 ± 8.9	0.001	PD-NC > PD-VAM
Digit Span Test (total)	13.9 ± 2.1	13.5 ± 1.9	12.0 ± 1.3	<0.001	PD-NC > PD-VAM; PD-EL > PD-VAM
Forward digit span	9.4 ± 1.3	9.2 ± 1.3	8.4 ± 0.8	<0.001	PD-NC > PD-VAM; PD-EL > PD-VAM
Backward digit span	4.5 ± 1.2	4.2 ± 1.0	3.6 ± 0.7	<0.001	PD-NC > PD-VAM; PD-EL > PD-VAM

executive function regulation, encompasses cognitive flexibility, decision-making, inhibition, and response selection<sup>28</sup>. Functional imaging studies have closely linked reduced DLPFC activation to executive function impairment<sup>13,14</sup>. The VLPFC and OFC, anatomically connected to the DLPFC, participate in behavioral inhibition, reward representation, decision-making, and memory processes, supporting information maintenance and retrieval in working memory<sup>28,29</sup>. IPL, a component of the central

executive network, plays a pivotal role in decision-making, goal execution, and top-down executive control<sup>30</sup>. Furthermore, the SMA, linked to the PFC, is implicated in advanced motor control and executive function integration<sup>31</sup>. Remarkably, repetitive transcranial magnetic stimulation (rTMS) applied to the PFC in individuals with mild cognitive impairment significantly improves executive functions and enhances PFC activation<sup>32</sup>. Thus, we posit that PFC functional dysregulation underlies the decline in



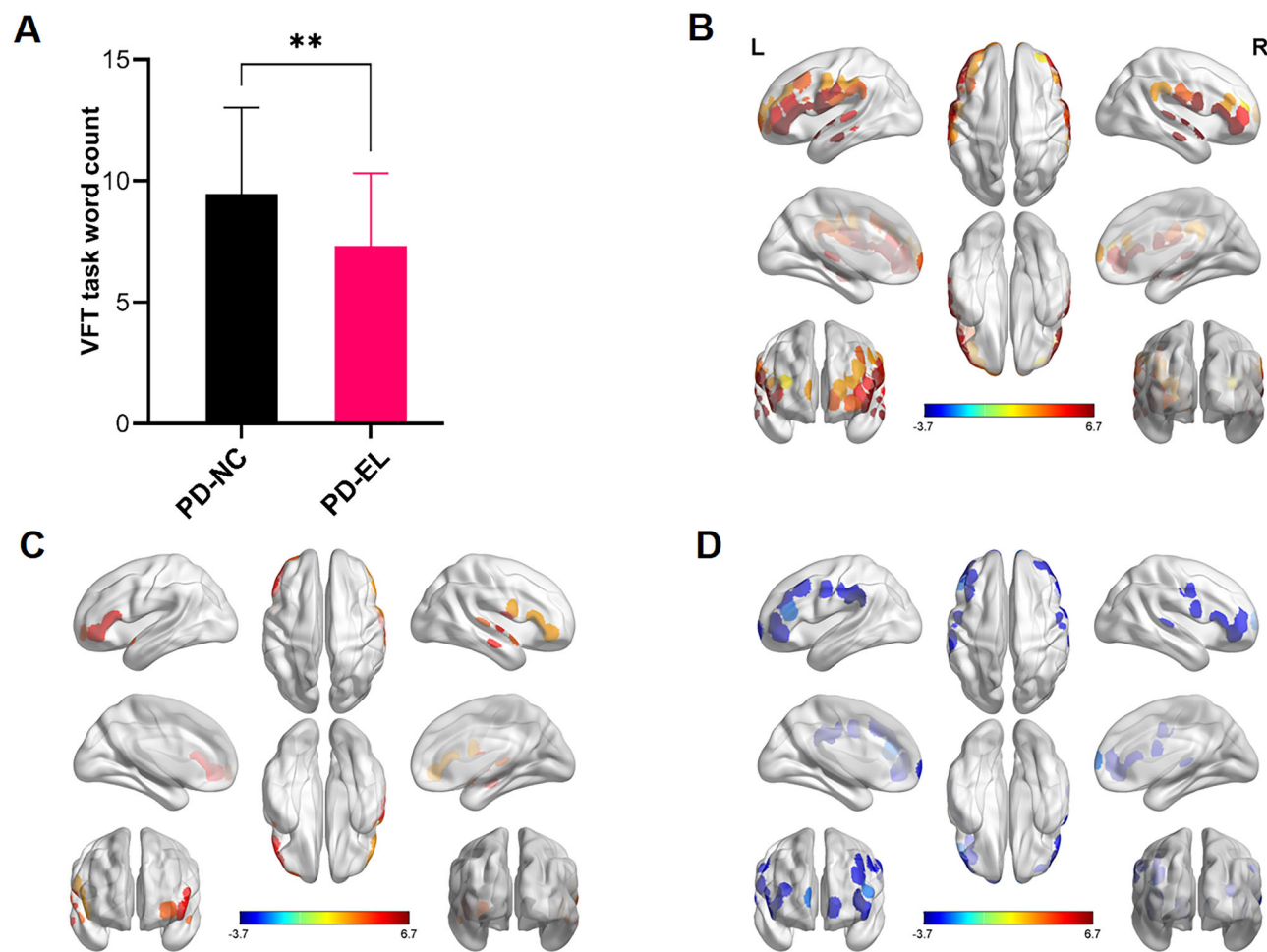


**Fig. 1 | Behavioral and neural activation characteristics of VFT in PD-NC and PD-EL subtype.** **A** PD-EL demonstrates a significant decrease in the number of generated words compared to PD-NC. **B** Cortical activity during VFT in PD-NC. **C** Cortical activity during VFT in PD-EL. **D** This panel shows the comparison between **B** and **C**, specifically indicating that reduced activity is observed in regions including DLPFC, VLPFC, SMA, left OFC, left IPL, and mPFC during VFT in PD-EL (**C**) patients compared to PD-NC (**B**). Error bars indicate standard deviation (s.d.). \*\* $p < 0.01$ . All brain activation results are significant at  $p < 0.05$ , FDR corrected.

**Table 4 | Regions of significant brain activity differences between groups in verbal fluency task and line orientation task under FDR correction**

	Channel	Side	Brain regions	T-value	P value
<b>Independent samples t-test:</b> PD-EL vs. PD-NC during verbal fluency task	8, 18, 25, 35, 39	Bilateral	Dorsolateral prefrontal cortex	-3.532 ~ -2.523	0.001 ~ 0.013
	23, 29, 34, 45, 50	Bilateral	Ventrolateral prefrontal cortex	-3.634 ~ -2.495	0.001 ~ 0.011
	48	Left	Orbitofrontal cortex	-2.613	0.011
	37	/	Medial prefrontal cortex	-2.490	0.015
	2, 9	Bilateral	Sensorimotor area	-2.572 ~ -2.553	0.012 ~ 0.013
	10, 21	Left	Inferior parietal lobule	-3.527 ~ -3.448	< 0.001
<b>RMANOVA:</b> PD-VAM vs. PD-NC during Line orientation task	34, 45, 50	Bilateral	Ventrolateral prefrontal cortex	-4.076 ~ -3.268	0.0001 ~ 0.016
	27	Left	Dorsolateral prefrontal cortex	-2.785	0.0066

Significance threshold set at  $p < 0.05$  (FDR-corrected).

executive abilities in PD-EL patients. Dysfunction in these brain regions hinders PD-EL patients’ recruitment of relevant areas, affecting their performance in tasks requiring response inhibition, memory retrieval, and top-down cognitive control, ultimately resulting in executive function deficits. Patients with PD commonly experience significant visual-spatial impairments, presenting a 60% higher risk compared to the general population, closely associated with poorer prognosis<sup>33</sup>. According to the dual syndrome hypothesis, compromised non-dopaminergic pathways (specifically cholinergic and noradrenergic systems) in the cerebral cortex

are believed to be the primary cause of visual-spatial impairments, along with cognitive deficits in attention and memory in PD-VAM patients<sup>7,8</sup>. Behavioral outcomes indicate that both condition type and patient group influence participants’ accuracy, with mutual interactions. Specifically, in the line orientation task, the PD-VAM group exhibited lower accuracy compared to the PD-NC group, while no significant differences were observed in the color naming task. This suggests that the disparity between groups primarily arises from the line orientation task, resulting in an interaction effect.

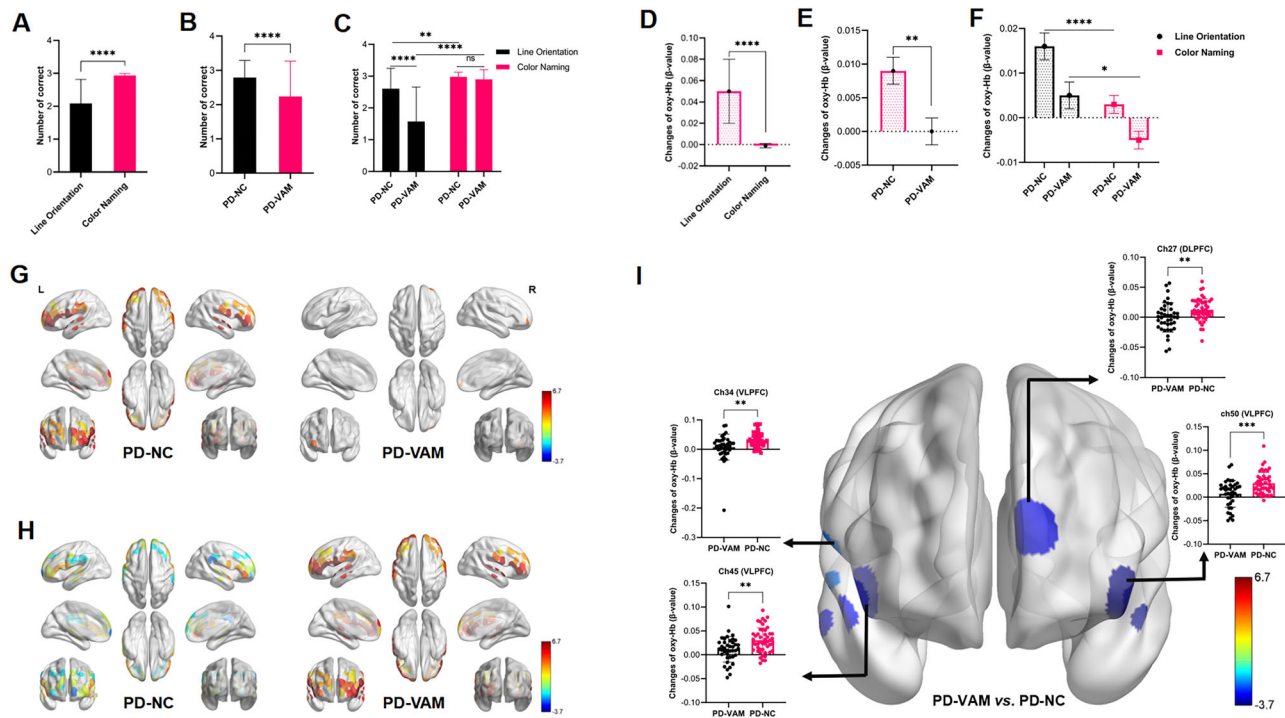


**Fig. 2 | Behavioral and neural features of LOT in PD-NC and PD-VAM subtype.** In behavioral RMANOVA, **A** Main effects of condition (Line Orientation and Color Naming), **B** main effects of group (PD-NC and PD-VAM), and **C** condition  $\times$  group interaction were significant observed. In the RMANOVA for brain activation, **D** main effects of condition and **E** main effects of group were significant, while **F** the interaction effect was not significant. **G** Cerebral activity during Line Orientation

condition in both groups; **H** cerebral activity during Color Naming condition in both groups; **I** reduced activity of VLPFC and DLPFC during the Line Orientation condition in PD-VAM patients compared to PD-NC. Error bars indicate standard deviation (s.d.). \* $p < 0.05$ , \*\* $p < 0.01$ , \*\*\*\* $p < 0.0001$ . All brain activation results are significant at  $p < 0.05$ , FDR corrected.

fNIRS results reveal significantly reduced brain activity in the VLPFC and DLPFC of the PD-VAM group, relative to the PD-NC group. The Domain-Specific hypothesis<sup>34</sup> posits that the VLPFC predominantly encodes visual shape information, while the DLPFC primarily encodes visual spatial information, forming an anatomical basis for this distinction. Subsequent research introduces the Integrative hypothesis<sup>35</sup>, suggesting that both the VLPFC and DLPFC regions are proficient in processing both spatial and shape information. A non-human primate study further demonstrates that visual spatial and shape information are conveyed through distinct visual pathways to the VLPFC and DLPFC, resulting in reciprocal interactions between these regions, leading to a comprehensive representation of visual spatial function in the PFC<sup>17</sup>.

Further investigation into the specific functions of the VLPFC and DLPFC in visual-spatial processing unveils pivotal roles. The VLPFC was found to play a critical role in spatial attention, exerting top-down feedback modulation on the visual cortex and prefrontal cortex<sup>36</sup>. Subsequent imaging and electrophysiological studies offer additional evidence for the crucial role of the VLPFC in visual-spatial attention<sup>36,37</sup>. Additionally, the DLPFC, anatomically adjacent to the VLPFC, is closely connected with the posterior parietal cortex responsible for processing visual spatial information<sup>16</sup>. Studies indicate the DLPFC's centrality in visual-spatial working memory function<sup>38</sup>, and in older individuals, reduced activation of the DLPFC during task execution<sup>39</sup>. rTMS of the DLPFC also affects performance in visual-spatial working memory tasks<sup>40</sup>. These findings emphasize the significance of the VLPFC and DLPFC in visual-spatial attention and working memory. This study observed diminished activation in the VLPFC and DLPFC of PD-VAM patients, indicating deficits in spatial attention and memory retrieval, ultimately impeding their ability to make effective judgments in tasks involving line orientation. Overall, our study, employing fNIRS technology and the LOT task, offers initial insights into the neural mechanisms underpinning visual-spatial dysfunction in PD-MCI patients,

revealing the roles of the VLPFC and DLPFC in the enigma of visual-spatial impairment in PD-MCI.

Our study demonstrates notable strengths. For the first time, we rigorously classified subtypes determined by the widely accepted and comprehensive Level II criteria<sup>1</sup> for the dual syndrome hypothesis, and collected cognitive data from healthy individuals in the same region as the patients. Guided by the dual syndrome hypothesis, we utilized fNIRS technology, known for its ecological validity and robustness against motion artifacts<sup>41</sup>, providing a thorough exploration of the neurobiological underpinnings of both PD-EL and PD-VAM subtypes. Lastly, employing a task-state paradigm, we simulated real-world neural activity patterns in PD-MCI patients, offering profound insights into the behavioral traits and neurobiological mechanisms underlying the onset of these subtypes.

This study has notable limitations. First, it did not include PD-MS patients, despite comprehensively investigating neurobiological mechanisms in the two PD-MCI subtypes according to the dual syndrome hypothesis. Future research should compare all three subtypes. Second, while no LEDD differences were found between groups<sup>14</sup>, potential effects of dopaminergic medications on brain function cannot be entirely ruled out. Third, this study did not measure premorbid intelligence levels, which might influence the interpretation of group differences. Fourth, while the visuospatial function test used in this study primarily assesses visuospatial abilities, it inevitably involves some executive function, which may limit the accuracy of our pure assessment of visuospatial capabilities. Future research should design more refined tasks to distinguish between the neural mechanisms of visuospatial and executive functions. Fifth, given the multidimensional nature of cognitive impairments in the PD-VAM subtype, future studies should explore the neural mechanisms of attention and memory and use statistical techniques (e.g., data-driven methods) to validate the subgroup classification and examine subtype differences. Sixth, while the TDDR algorithm effectively handles motion artifacts in fNIRS

data, it may not cover all types. To address this, we will implement wavelet filtering<sup>42</sup>, especially for low-frequency, low-amplitude artifacts, to enhance data accuracy and robustness. Lastly, the cross-sectional design limits our ability to track changes over time in cognitive function, behavior, and neurobiological mechanisms. Future studies could benefit from a longitudinal approach.

Our study fills a crucial gap in PD-MCI research by examining task-related activation patterns in PD-MCI subtypes, diverging from the predominant focus on resting-state brain activity. Using fNIRS, our data suggest that PD-EL patients may exhibit reduced activation across a network including the DLPFC, VLPFC, SMA, mPFC, left OFC, and left IPL during executive tasks, whereas PD-VAM patients may show diminished activation primarily in the VLPFC and left DLPFC during visuospatial tasks relative to PD-NC. Notably, there is some cross-domain overlap in the cognitive tests, and the task design may introduce mixed activation effects, factors which may affect the precise differentiation of activation patterns. Therefore, while our results indicate differential neural activation patterns, they should be regarded as promising preliminary evidence. These insights shed light on the neural underpinnings of cognitive dysfunction in PD-MCI and emphasize the potential for developing targeted, subtype-specific interventions.

## Methods

### Participants

For this investigation, 202 participants were enrolled, comprising 142 PD patients and 60 healthy individuals. Notably, 20 PD patients were excluded due to the presence of mixed cognitive impairment (see classification of subtypes of mild cognitive impairment section). The participants were drawn from the Movement Disorders Unit, outpatient clinics at the First Hospital of Dalian Medical University, as well as the surrounding communities. Inclusion criteria for PD patients followed the 2015 diagnostic guidelines proposed by the International Parkinson and Movement Disorder Society (MDS)<sup>43</sup>, which included right-handedness, the ability to independently complete scale assessments, and good visual and auditory acuity (or corrected vision/hearing). Exclusion criteria consisted of patients diagnosed with PDD according to the 2007 MDS guidelines<sup>44</sup>, a history of severe psychiatric or neurological disorders affecting brain function, significant medical conditions, substance abuse, and patients who had undergone deep brain stimulation.

### Characteristics and clinical measures

We recorded participants' age, gender, years of education, and BMI. Disease duration for PD was documented, and all anti-PD medications were recorded and converted to levodopa equivalent daily doses (LEDD)<sup>45</sup>. Motor symptom intensity was conducted utilizing the Movement Disorder Society Unified Parkinson's Disease Rating Scale Part III (MDS-UPDRS III)<sup>46</sup>, while disease severity was evaluated using the Hoehn and Yahr staging. Anxiety and depression symptom severity were evaluated using the 14-item Hamilton Anxiety Rating Scale (HAMA) and the 24-item Hamilton Depression Rating Scale (HAMD), respectively.

### Local healthy individuals' cognitive proficiency

According to Level II criteria, cognitive screening should deviate 1–2 standard deviations below norms for typical cognition<sup>1</sup>. Previous studies often relied on published norms, but limitations exist: (1) Regional differences impact cognitive function<sup>47</sup>; (2) Data may be outdated due to lifestyle changes and improved chronic disease management; (3) Demographic information misalignment may occur. Therefore, we collected psychological data from 60 demographically-matched healthy individuals in the same region as the patients. Calculating their average performance across different cognitive domains enhances PD-MCI diagnosis accuracy and subtyping.

### Neuropsychological evaluation

Participants completed a comprehensive neuropsychological assessment, which encompassed the Montreal Cognitive Assessment (MOCA) for a

comprehensive evaluation of global cognition. Following MDS's 2012 Level II criteria for PD-MCI<sup>1</sup>, standardized tests were administered to assess five cognitive domains: (1) Executive functions using the Clock Drawing Test<sup>48</sup> and Category Fluency Test (animals)<sup>49</sup>; (2) Language functions with the Boston Naming Test<sup>50</sup> and Similarities Test<sup>51</sup>; (3) Visuospatial functions employing Clock copying (Royall's CLOX2)<sup>52</sup> and Block Design Test<sup>51</sup>, based on its use in previous PD-MCI studies<sup>53,54</sup> as a tool for assessing visuospatial functions; (4) Attention functions via the Symbol Digit Test<sup>51</sup> and Digit Span Test<sup>51</sup>; and (5) Memory functions assessed by Logical Memory<sup>55</sup> and Auditory Verbal Learning Test<sup>56</sup>. Assessments and examinations were performed in the "on" phase for patients experiencing "on-off" phenomena.

### Classification of subtypes of mild cognitive impairment

Following the MDS's 2012 Level II criteria for PD-MCI, once cognitive decline was identified, each cognitive domain underwent dual testing. The diagnosis of PD-MCI involved abnormalities in a minimum of two neuropsychological assessments, which could manifest within a single domain or across multiple domains<sup>1</sup>. The criteria included a deviation of 1.5 standard deviations below norms for typical cognition, and the absence of PDD<sup>1</sup>.

Based on the dual syndrome hypothesis<sup>6–8,57</sup>, two distinct cognitive subtypes were identified among PD-MCI patients: (1) PD-EL subtype, associated with disruptions in dopaminergic-dependent neural pathways, resulting in impairments in executive and/or language functions, without affecting visuospatial, attentional, and memory functions. Language functions closely relate to executive functions<sup>58</sup>, and in early-stage PD cognitive impairment, language deficits often represent part of dysexecutive syndrome<sup>8,57</sup>, hence incorporating it into the PD-EL subtype; (2) PD-VAM subtype, attributed to impairments in non-dopaminergic pathways (involving the cholinergic and noradrenergic systems), resulting in deficits in visuospatial, attention, and/or memory functions, while executive and language functions remain intact. Additionally, normal cognition (PD-NC) is characterized by no impairments in cognitive domains. Given the study's specific focus on precisely evaluating neurobiological differences between PD-EL and PD-VAM subtypes under the dual syndrome hypothesis, we did not include mixed subtypes (PD-MS) characterized by concurrent impairments in visuospatial, attentional, or memory functions along with executive or language deficits, in this research, resulting in the exclusion of 20 participants.

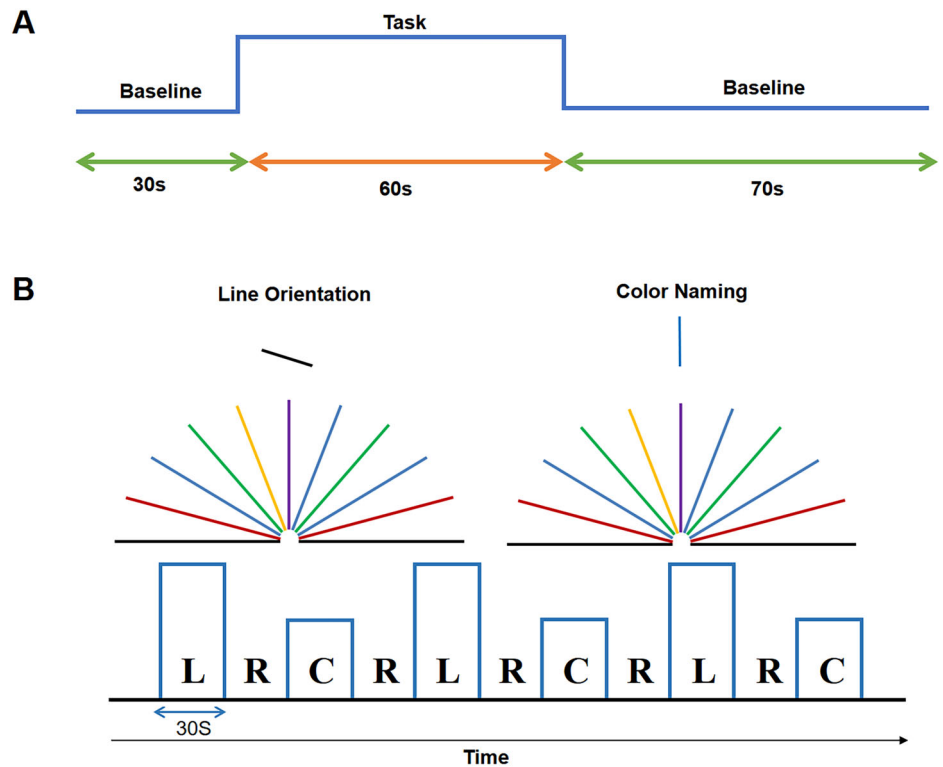
### Verbal fluency task

Following MDS's 2012 PD-MCI guidelines for cognitive domain assessment, the verbal fluency task (VFT) was utilized to evaluate executive functions in both PD-EL subtype and PD-NC<sup>1</sup>, mirroring a previously described task process<sup>14</sup>. The test encompassed three phases: a 30-s pre-task phase, a 70-s post-task phase, and a 60-s task phase (comprising three 20-s blocks). Patients verbally counted numbers 1 to 5 during both pre-task and post-task baseline periods (Fig. 3A). In the 60-s task phase, the screen displayed three Chinese characters: 河 (meaning river), 日 (meaning day), and 家 (meaning home), each with a 20-s time limit. Patients were instructed to verbally generate phrases from each provided word as many times as possible. The total correct word count served as the VFT behavioral data.

### Line orientation task

The Line Orientation Task (LOT) assessed visuospatial function<sup>16</sup> in both PD-VAM subtype and PD-NC, following MDS's 2012 PD-MCI guidelines<sup>1</sup>. Given the unique precursor visuospatial deficits in the non-dopaminergic subtype<sup>7</sup>, we assessed visuospatial function in the PD-VAM subtype using the LOT task. E-prime software controlled stimulus presentation, with a 10-s wait period to minimize task interference. Participants were instructed to focus solely on the current task and relax afterwards, enhancing focus and improving the accuracy of the data collected. The LOT included experimental and control conditions (Fig. 3B). In the experimental condition (Line Orientation), participants identified and verbally stated the direction (left or

**Fig. 3 | Tasks employed in this study.** **A** Verbal Fluency Task (VFT) assesses executive function. **B** Line Orientation Task (LOT) evaluates visuospatial function. L line orientation, R rest, C color naming.



right) and color of the lower line matching the orientation of the example line above. The control condition involved Color Naming, where participants stated the color of the example line. Participant responses were recorded as behavioral data. The experiment comprised three 30-s blocks of Line Orientation and Color Naming conditions, alternating with a 30-s resting period after each task (10 s before the first task and 20 s after the last task), totaling 360 s. Each block was designed to emphasize a single, extended task period, ensuring thorough engagement and capturing a complete hemodynamic response cycle.

#### fNIRS data acquisition

A 52-channel fNIRS system (ETG-4000, Hitachi Medical Corp., Japan) with a 0.1-s temporal resolution and a sampling rate of 10 Hz was employed. This system, based on an enhanced Beer-Lambert law, employed two wavelengths (695 nm and 830 nm) to measure oxy-hemoglobin ([oxy-Hb]) and deoxy-hemoglobin (deoxy-Hb). It comprised 17 emission and 16 receiver probes in a  $3 \times 11$  array, spaced 3.0 cm apart. Probes, following the international 10-20 system, were positioned on the subject's forehead and scalp, with the lowest probe along the T4-Fpz-T3 line. A virtual registration method, based on the same system, established correspondence between channels and cortical locations<sup>59</sup>. Detailed coordinates for fNIRS channels were from Takizawa et al. (2014)<sup>60</sup>. The measured brain regions, as shown in Supplementary Fig. 1, included DLPFC [channels (Ch) 3, 4, 7, 8, 14, 15, 17, 18, 25, 26, 27, 28, 35, 36, 38, and 39], VLPFC (Ch 13, 19, 23, 24, 29, 30, 34, 40, 45, and 50), Medial Prefrontal Cortex (mPFC) (Ch 5, 6, 16, and 37), Orbitofrontal Cortex (OFC) (Ch 46, 47, 48, and 49), Temporal Lobe (TL) (Ch 32, 33, 41, 42, 43, 44, 51, and 52), Supplementary Motor Area (SMA) (Ch 2, 9, 12, 20, 22, and 31), and Inferior Parietal Lobule (IPL) (Ch 1, 10, 11, and 21), aligning with previous fNIRS investigations<sup>13,14,61</sup>. In our study, fNIRS channels in each region of interest were combined using a simple average to assess overall activation levels.

#### Ethics approval and informed consent

This study was approved by the Ethics Committee of the First Hospital of Dalian Medical University (Approval No. PJ-KS-KY-2021-218). Written

informed consent was obtained from all participants before their enrollment in the study.

#### Statistical analyses

Demographic and clinical data underwent analysis through SPSS 26.0. Continuous variables were denoted as mean  $\pm$  standard deviation, while categorical variables were represented as counts (n) and percentages (%). Gender comparisons employed the chi-square ( $\chi^2$ ) test. Normality was assessed with Shapiro-Wilk for  $n \leq 50$  and Kolmogorov-Smirnov for  $n > 50$ . For other indicators, we used independent  $t$  tests or one-way ANOVA if normality was met, or Mann-Whitney U or Kruskal-Wallis tests if not. Significance was set at  $p < 0.05$ .

The raw data from two task states were preprocessed with the NIRS-KIT toolbox<sup>62</sup> in MATLAB. Emphasis was placed on [oxy-Hb] levels due to their direct reflection of cognitive activity and alignment with fMRI BOLD signals<sup>23</sup>. The modified Lambert-Beer law converted fNIRS light data to [oxy-Hb] concentrations. Data were detrended to remove linear baseline drift, and head motion correction employed the Time Derivative Distribution Repair (TDDR) algorithm<sup>63</sup>. A bandpass Butterworth filter (0.006–0.2 Hz) eliminated irrelevant frequency components.

During the VFT, we employed a General Linear Model (GLM) to analyze oxygenated hemoglobin changes in each participant across channels. Task conditions were convolved with the standard hemodynamic response function (HRF) within the GLM, producing corresponding regressors. The baseline included the final 10 s of the pre-task phase and 5 s after 50 s of the post-task phase<sup>14</sup>. GLM parameters were computed for each channel, yielding  $\beta$ -values for specific conditions<sup>62</sup>. The task-related  $\beta$ -value represents the difference between word generation and baseline. One-sample and independent sample  $t$ -tests compared  $\beta$ -values for PD-NC and PD-EL groups. Inter-group disparities in VFT behavioral data were assessed with independent sample  $t$  tests. The results underwent multiple comparison correction, considering significance at  $p < 0.05$ .

In the LOT, [oxy-Hb] changes were assessed using a GLM across channels. Task stimuli were convolved with the standard HRF in the GLM, generating regressors. The experiment included three blocks each of Line



Orientation and Color Naming conditions, with each block lasting 60 s (comprising a 10-s baseline, 30 s of task activation, and 20 s of rest). For the Line Orientation task, the GLM was applied to these blocks to obtain task-related  $\beta$ -values, which represent the change in [oxy-Hb] during task activation relative to the baseline. The baseline was defined as the initial 10 s before task activation in each block, serving as a reference point for subsequent changes. The  $\beta$ -values were then calculated for each channel based on the difference in [oxy-Hb] between the task activation period and the baseline. The Color Naming task followed the same procedure. Brain imaging data underwent analysis through a repeated measure analysis of variance (RMANOVA) based on whole-brain activation, considering factors like group (PD-NC and PD-VAM), condition type (Line Orientation and Color Naming task), and channel category (52 channels). Main effects, interaction effects, and simple effects were assessed. Corrections for degrees of freedom (df) and p-values were based on Mauchly's sphericity test. Partial  $\eta^2$  was used for effect size. Behavioral data also underwent RMANOVA. Statistical analysis was performed employing SPSS 26.0 and NIRS\_KIT software. Results underwent correction for multiple comparisons, with significance established at  $p < 0.05$  (two-tailed).

## Data availability

The datasets generated and/or analyzed during the current study are not publicly available due to privacy concerns for research participants but are available from the corresponding author on reasonable request. Restrictions may be applied to sensitive data for privacy protection.

Received: 23 April 2024; Accepted: 6 May 2025;

Published online: 12 June 2025

## References

- Litvan, I. et al. Diagnostic criteria for mild cognitive impairment in Parkinson's disease: Movement Disorder Society Task Force guidelines. *Mov. Disord.* **27**, 349–356 (2012).
- Monastero, R. et al. Mild cognitive impairment in Parkinson's disease: the Parkinson's disease cognitive study (PACOS). *J. Neurol.* **265**, 1050–1058 (2018).
- Santangelo, G. et al. Mild cognitive impairment in newly diagnosed Parkinson's disease: A longitudinal prospective study. *Parkinsonism Relat. Disord.* **21**, 1219–1226 (2015).
- Hoogland, J. et al. Mild cognitive impairment as a risk factor for Parkinson's disease dementia. *Mov. Disord.* **32**, 1056–1065 (2017).
- Hely, M. A., Reid, W. G., Adena, M. A., Halliday, G. M. & Morris, J. G. The Sydney multicenter study of Parkinson's disease: the inevitability of dementia at 20 years. *Mov. Disord.* **23**, 837–844 (2008).
- Kehagia, A. A., Barker, R. A. & Robbins, T. W. Neuropsychological and clinical heterogeneity of cognitive impairment and dementia in patients with Parkinson's disease. *Lancet Neurol.* **9**, 1200–1213 (2010).
- Kehagia, A. A., Barker, R. A. & Robbins, T. W. Cognitive impairment in Parkinson's disease: the dual syndrome hypothesis. *Neurodegener. Dis.* **11**, 79–92 (2013).
- Gratwicke, J., Jahanshahi, M. & Foltynie, T. Parkinson's disease dementia: a neural networks perspective. *Brain* **138**, 1454–1476 (2015).
- Lang, S. et al. Network basis of the dysexecutive and posterior cortical cognitive profiles in Parkinson's disease. *Mov. Disord.* **34**, 893–902 (2019).
- Devignes, Q. et al. Resting-State Functional Connectivity in Frontostriatal and Posterior Cortical Subtypes in Parkinson's Disease-Mild Cognitive Impairment. *Mov. Disord.* **37**, 502–512 (2022).
- Betrouni, N. et al. The frontostriatal subtype of mild cognitive impairment in Parkinson's disease, but not the posterior cortical one, is associated with specific EEG alterations. *Cortex* **153**, 166–177 (2022).
- Brandão, P. R. P. et al. Cognitive impairment in Parkinson's disease: A clinical and pathophysiological overview. *J. Neurol. Sci.* **419**, 117177 (2020).
- Wang, H. Y. et al. The impact of anxiety on the cognitive function of informal Parkinson's disease caregivers: Evidence from task-based and resting-state fNIRS. *Front. Psychiatry* **13**, 960953 (2022).
- Wang, H. Y. et al. Effects of trihexyphenidyl on prefrontal executive function and spontaneous neural activity in patients with tremor-dominant Parkinson's disease: An fNIRS study. *Parkinsonism Relat. Disord.* **105**, 96–102 (2022).
- Devignes, Q. et al. Posterior Cortical Cognitive Deficits Are Associated With Structural Brain Alterations in Mild Cognitive Impairment in Parkinson's Disease. *Front. Aging Neurosci.* **13**, 668559 (2021).
- Zeller, J. B. et al. Altered parietal brain oxygenation in Alzheimer's disease as assessed with near-infrared spectroscopy. *Am. J. Geriatr. Psychiatry* **18**, 433–441 (2010).
- Tang, H. et al. Reward-related choices determine information timing and flow across macaque lateral prefrontal cortex. *Nat. Commun.* **12**, 894 (2021).
- Constantinidis, C. & Qi, X. L. Representation of spatial and feature information in the monkey dorsal and ventral prefrontal cortex. *Front. Integr. Neurosci.* **12**, 31 (2018).
- Chan, A. W. Functional organization and visual representations of human ventral lateral prefrontal cortex. *Front. Psychol.* **4**, 371 (2013).
- Müller, N. G., Machado, L. & Knight, R. T. Contributions of subregions of the prefrontal cortex to working memory: evidence from brain lesions in humans. *J. Cogn. Neurosci.* **14**, 673–686 (2002).
- Clark, K., Squire, R. F., Merrihki, Y. & Noudoost, B. Visual attention: Linking prefrontal sources to neuronal and behavioral correlates. *Prog. Neurobiol.* **132**, 59–80 (2015).
- Pinti, P. et al. The present and future use of functional near-infrared spectroscopy (fNIRS) for cognitive neuroscience. *Ann. NY Acad. Sci.* **1464**, 5–29 (2020).
- Sato, H. et al. A NIRS-fMRI investigation of prefrontal cortex activity during a working memory task. *Neuroimage* **83**, 158–173 (2013).
- Pu, L. et al. Greater prefrontal activation during sitting toe tapping predicts severe freezing of gait in Parkinson's disease: an fNIRS study. *Cereb. Cortex* **33**, 959–968 (2023).
- Galtier, I. et al. Mild cognitive impairment in Parkinson's disease: Clustering and switching analyses in verbal fluency test. *J. Int. Neuropsychol. Soc.* **23**, 511–520 (2017).
- Simonet, C. et al. The motor prodromes of Parkinson's disease: From bedside observation to large-scale application. *J. Neurol.* **268**, 2099–2108 (2021).
- Diamond, A. Executive functions. *Annu. Rev. Psychol.* **64**, 135–168 (2013).
- Elliott, R. Executive functions and their disorders. *Br. Med. Bull.* **65**, 49–59 (2003).
- Rudebeck, P. H. & Rich, E. L. Orbitofrontal cortex. *Curr. Biol.* **28**, R1083–R1088 (2018).
- Menon, V. Large-scale brain networks and psychopathology: A unifying triple network model. *Trends Cogn. Sci.* **15**, 483–506 (2011).
- Seeger, C. A. The visual corticostriatal loop through the tail of the caudate: Circuitry and function. *Front. Syst. Neurosci.* **7**, 104 (2013).
- Chou, Y. H., Ton That, V. & Sundman, M. A systematic review and meta-analysis of rTMS effects on cognitive enhancement in mild cognitive impairment and Alzheimer's disease. *Neurobiol. Aging* **86**, 1–10 (2020).
- Hamedani, A. G. et al. Visual impairment is more common in Parkinson's disease and is a risk factor for poor health outcomes. *Mov. Disord.* **35**, 1542–1549 (2020).
- Wilson, F. A., Scailidhe, S. P. & Goldman-Rakic, P. S. Dissociation of object and spatial processing domains in primate prefrontal cortex. *Science* **260**, 1955–1958 (1993).
- Miller, E. K. & Cohen, J. D. An integrative theory of prefrontal cortex function. *Annu. Rev. Neurosci.* **24**, 167–202 (2001).
- Meyyappan, S. et al. Top-down control of the left visual field bias in cued visual spatial attention. *Cereb. Cortex* **33**, 5097–5107 (2023).

37. Sapountzis, P. et al. Dynamic and stable population coding of attentional instructions coexist in the prefrontal cortex. *Proc. Natl. Acad. Sci. USA* **119**, e2202564119 (2022).
38. Sommer, M. A. & Wurtz, R. H. Composition and topographic organization of signals sent from the frontal eye field to the superior colliculus. *J. Neurophysiol.* **83**, 1979–2001 (2000).
39. Kronovsek, T. et al. Age-related decline in visuo-spatial working memory is reflected by dorsolateral prefrontal activation and cognitive capabilities. *Behav. Brain Res.* **398**, 112981 (2021).
40. Oliveri, M. et al. Parieto-frontal interactions in visual-object and visual-spatial working memory: evidence from transcranial magnetic stimulation. *Cereb. Cortex* **11**, 606–618 (2001).
41. Cui, X. et al. A quantitative comparison of NIRS and fMRI across multiple cognitive tasks. *Neuroimage* **54**, 2808–2821 (2011).
42. Brigadoi, S. et al. Motion artifacts in functional near-infrared spectroscopy: a comparison of motion correction techniques applied to real cognitive data. *Neuroimage* **85**, 181–191 (2014).
43. Postuma, R. B. et al. MDS clinical diagnostic criteria for Parkinson's disease. *Mov. Disord.* **30**, 1591–1601 (2015).
44. Emre, M. et al. Clinical diagnostic criteria for dementia associated with Parkinson's disease. *Mov. Disord.* **22**, 1689–1707 (2007).
45. Tomlinson, C. L. et al. Systematic review of levodopa dose equivalency reporting in Parkinson's disease. *Mov. Disord.* **25**, 2649–2653 (2010).
46. Goetz, C. G. et al. Movement Disorder Society-sponsored revision of the Unified Parkinson's Disease Rating Scale (MDS-UPDRS): scale presentation and clinimetric testing results. *Mov. Disord.* **23**, 2129–2170 (2008).
47. Wang, Y. et al. Education, neighborhood environment, and cognitive decline: Findings from two prospective cohort studies of older adults in China. *Alzheimers Dement* **19**, 560–568 (2023).
48. Sunderland, T. et al. Clock drawing in Alzheimer's disease: A novel measure of dementia severity. *J. Am. Geriatr. Soc.* **37**, 725–729 (1989).
49. Lima, I. M. M., Peckham, A. D. & Johnson, S. L. Cognitive deficits in bipolar disorders: implications for emotion. *Clin. Psychol. Rev.* **59**, 126–136 (2018).
50. Chen, T. B. et al. Culture qualitatively but not quantitatively influences performance in the Boston naming test in a Chinese-speaking population. *Dement. Geriatr. Cogn. Dis. Extra* **4**, 86–94 (2014).
51. Gong, Y. Wechsler Adult Intelligence Scale-Revised in China Version (Changsha, 1992).
52. Royall, D. R., Cordes, J. A. & Polk, M. CLOX: an executive clock drawing task. *J. Neurol. Neurosurg. Psychiatry* **64**, 588–594 (1998).
53. Wang, W. et al. Changes of brain structural network connection in Parkinson's disease patients with mild cognitive dysfunction: a study based on diffusion tensor imaging. *J. Neurol.* **267**, 933–943 (2020).
54. Jiang, Z. et al. Characterization of a pathogenic variant in GBA for Parkinson's disease with mild cognitive impairment patients. *Mol. Brain* **13**, 102 (2020).
55. Gong, Y. Manual of Wechsler Memory Scale-Chinese Version (Changsha, 1989).
56. Zhao, Q., Lv, Y., Zhou, Y., Hong, Z. & Guo, Q. Short-term delayed recall of auditory verbal learning test is equivalent to long-term delayed recall for identifying amnesic mild cognitive impairment. *PLoS One* **7**, e51157 (2012).
57. Hirano, S. Clinical implications for dopaminergic and functional neuroimage research in cognitive symptoms of Parkinson's disease. *Mol. Med.* **27**, 40 (2021).
58. Lowit, A. et al. Task-based profiles of language impairment and their relationship to cognitive dysfunction in Parkinson's disease. *PLoS One* **17**, e0276218 (2022).
59. Tsuzuki, D. et al. Virtual spatial registration of stand-alone fNIRS data to MNI space. *Neuroimage* **34**, 1506–1518 (2007).
60. Takizawa, R. et al. Neuroimaging-aided differential diagnosis of the depressive state. *Neuroimage* **85**, 498–507 (2014).
61. Sakakibara, E. et al. Detection of resting state functional connectivity using partial correlation analysis: A study using multi-distance and whole-head probe near-infrared spectroscopy. *Neuroimage* **142**, 590–601 (2016).
62. Hou, X. et al. NIRS-KIT: a MATLAB toolbox for both resting-state and task fNIRS data analysis. *Neurophotonics* **8**, 010802 (2021).
63. Fishburn, F. A. et al. Temporal derivative distribution repair (TDDR): A motion correction method for fNIRS. *Neuroimage* **184**, 171–179 (2019).

## Acknowledgements

This work was supported by the Ph.D. Research Fund of Jining No. 1 People's Hospital (Grant No. 2024-BS-003), the Medical and Health Science and Technology Project of Shandong Province (Grant No. 202403090535), the Key R&D Program of Jining (Major Program, Grant No. 2023YXNS004), and the Dalian Medical Science Research Program Project (Grant No. 1812009).

## Author contributions

H.-Y.W.: Data curation, Formal analysis, Funding acquisition, Investigation, Methodology, Visualization, Writing—original draft, and Writing—review & editing. L.R.: Data curation, Writing—review & editing. Z.Y.: Writing—review & editing. T.Z.: Data curation, Visualization, Writing—review & editing. Z.L.: Data curation, Conceptualization, Formal Analysis, Supervision, Project administration, Validation, Funding acquisition, Writing—review & editing. All authors take responsibility for the accuracy and integrity of the work. All authors read and approved the final manuscript.

## Competing interests

The authors declare no competing interests.

## Additional information

**Supplementary information** The online version contains supplementary material available at <https://doi.org/10.1038/s41531-025-01013-z>.

**Correspondence** and requests for materials should be addressed to Tingting Zhou or Zhanhua Liang.

**Reprints and permissions information** is available at <http://www.nature.com/reprints>

**Publisher's note** Springer Nature remains neutral with regard to jurisdictional claims in published maps and institutional affiliations.

**Open Access** This article is licensed under a Creative Commons Attribution-NonCommercial-NoDerivatives 4.0 International License, which permits any non-commercial use, sharing, distribution and reproduction in any medium or format, as long as you give appropriate credit to the original author(s) and the source, provide a link to the Creative Commons licence, and indicate if you modified the licensed material. You do not have permission under this licence to share adapted material derived from this article or parts of it. The images or other third party material in this article are included in the article's Creative Commons licence, unless indicated otherwise in a credit line to the material. If material is not included in the article's Creative Commons licence and your intended use is not permitted by statutory regulation or exceeds the permitted use, you will need to obtain permission directly from the copyright holder. To view a copy of this licence, visit <http://creativecommons.org/licenses/by-nc-nd/4.0/>.

© The Author(s) 2025